Published online 18 September 2007 *Nucleic Acids Research, 2007, Vol. 35, No. 19* **6357–6366**
doi:10.1093/nar/gkm692

The role of peptide motifs in the evolution of a protein network

Hirohide Saito[1–4,*], Shunnichi Kashida[3], Tan Inoue[3,4] and Kiyotaka Shiba[1,2,*]

[1]Department of Protein Engineering, Cancer Institute, Japanese Foundation for Cancer Research, Koto-ku, Tokyo 135-8550, [2]CREST, Japan Science and Technology Corporation (JST), Kawaguchi Center Building 4-1-8, Honcho, Kawaguchi-shi, Saitama 332-0012, [3]Laboratory of Gene Biodynamics, Graduate School of Biostudies, Kyoto University, Oiwake-cho, Kitashirakawa, Sakyo-ku, Kyoto, 606-8502 and [4]ICORP, JST, Kawaguchi Center Building 4-1-8, Honcho, Kawaguchi-shi, Saitama 332-0012, Japan

Received April 17, 2007; Revised August 21, 2007; Accepted August 22, 2007

ABSTRACT

Naturally occurring proteins in cellular networks often share peptide motifs. These motifs have been known to play a pivotal role in protein interactions among the components of a network. However, it remains unknown how these motifs have contributed to the evolution of the protein network. Here we addressed this issue by a synthetic biology approach. Through the motif programming method, we have constructed an artificial protein library by mixing four peptide motifs shared among the Bcl-2 family proteins that positively or negatively regulate the apoptosis networks. We found one strong pro-apoptotic protein, d29, and two proteins having moderate, but unambiguous anti-apoptotic functions, a10 and d16, from the 28 tested clones. Thus both the pro- and anti-apoptotic modulators were present in the library, demonstrating that functional proteins with opposing effects can emerge from a single pool prepared from common motifs. Motif programming studies have exhibited that the annotated function of the motifs were significantly influenced by the context that the motifs embedded. The results further revealed that reshuffling of a set of motifs realized the promiscuous state of protein, from which disparate functions could emerge. Our finding suggests that motifs contributed to the plastic evolvability of the protein network.

INTRODUCTION

Protein regulatory networks that underlie various cell activities have evolved with an autonomy and robustness (1,2). The proteins that comprise regulatory networks often share peptide motifs, a short conserved amino acid sequence (3,4). Recently, with advent of high-throughput proteomics, the identification of peptide motifs has been drastically accelerated (5,6). Motifs are often associated with biological functions, protein structures or evolutionary history, and generally consist of short amino acids (typically 5–25 amino acids). It has been reported that several peptide motifs lose original biological functions when they are isolated from their parental proteins, indicating that peptide motifs are capricious, as they are strongly influenced by their context within the proteins (7,8). In contrast, protein domains often fold independently of the rest of the protein chain, and typically consist of more than 25 amino acids.

Some peptide motifs in a protein network have been shown to be involved in the protein–protein interaction in the network (9) thus they have a pivotal role in the dynamics of the network (10,11) (Figure 1A). However, it remains unknown how these motifs have contributed to the evolution of the protein network. In this study, we addressed this question by a synthetic biology approach (12), in which a library of artificial proteins was created from a combinatorial assembly of extant peptide motifs in the apoptosis network and the pro- and anti-apoptotic clones were searched from the library. We took synthetic biology approach to investigate the role of peptide motifs in the evolution of protein networks. Although the classical top-down approach (i.e. the analyses of natural proteins with a variety of combination of motifs; as shown in Figure 1B) is crucial to elucidate the relationship between motifs and protein functions, it is difficult to investigate whether the reshuffling of a set of motifs can drastically change protein functions/localizations by interfering with naturally occurring protein networks. Thus we chose our motif programming approach to generate such a motif-mixing protein library (12).

The peptide motifs we have been focusing on included the BH1, BH2, BH3 and BH4 motifs, the combinations of

*To whom correspondence should be addressed. Tel: +81 3 3570 0489; Fax: +81 3 3570 0461; Email: kshiba@jfcr.or.jp
Correspondence may also be addressed to Hirohide Saito. Tel: +81 75 753 3997; Fax: +81 75 753 3996; Email: saito@lif.kyoto-u.ac.jp

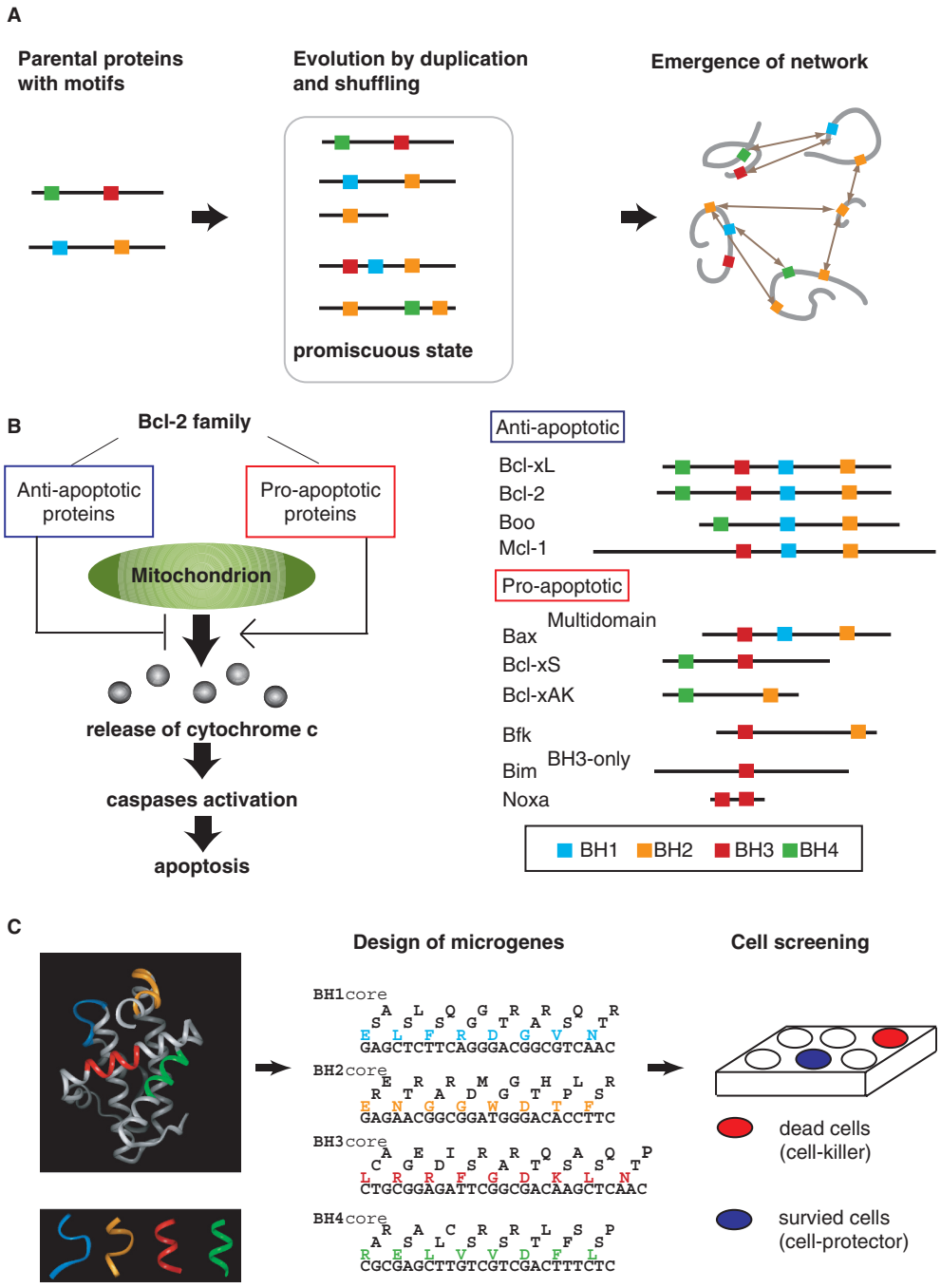

Figure 1. Exploring apoptotic regulatory networks by motif programming. (**A**) Schematic diagram of the roles of motifs in network evolution and network dynamics. (**B**) (left) Apoptotic regulatory networks regulated by Bcl-2 family proteins. (right) Both anti-apoptotic and pro-apoptotic proteins share the BH1-4 peptide motifs but the proteins vary with respect to the number of the four motifs. (**C**) Screening strategy of cell death modulators utilized in this study. (left) Structure of human Bcl-xL, an anti-apoptotic multidomain protein [based on the (1R2D)]. The core regions of the BH1, BH2, BH3 and BH4 motifs focused on in this study are shown in cyan, orange, red and green, respectively, though we used the BH3 motif from Noxa instead of Bcl-xL. (middle) Four designed microgenes that encode BH peptides in their first reading frames. (right) Cell-based screening to identify artificial cell death modulators that oppositely regulate the apoptotic circuits (cell-killer or cell-protector).

which are conserved in the Bcl-2 family proteins of the mitochondria-dependent apoptosis network (13–15). The Bcl-2 family proteins are classified as 'pro-apoptotic' or 'anti-apoptotic' depending on their roles (Figure 1B, left). The members are further divided into three classes based on the BH1-4 motifs they contain (Figure 1B, right); (i) multidomain members contain all four BH motifs (Bcl-xL, Bcl-2, etc.). The members act as an anti-apoptotic factor, (ii) multidomain members (Bax, Bak, etc.) that are pro-apoptotic proteins and (iii) pro-apoptotic BH3-only members (Bim, Noxa, etc.). As a first approximation, the motifs BH3 and BH4 are linked with the pro- and

anti-apoptotic phenotypes, respectively. In fact, experiments with synthetic peptides have shown that BH3 and BH4 acted as apoptosis-inducing and apoptosis-protecting agents, respectively (16–19). However, recent findings are more equivocal. For example, Bcl-xL and Bcl-xS share the same BH3-4 motifs in their structures, however, the former acts as an anti-factor and the latter acts as a pro-factor (Figure 1B, right). It has also been reported that Bcl-2 has a dual role as both a cell protector and a killer and that the ability to switch roles depends on the Bcl-2's subcellular localization (20,21). These facts indicated that each motif did not directly link with the specific function. Our previous study has also revealed the capriciousness of the phenotype–genotype linkage of BH3 (7). Among the artificial proteins containing BH3, only some clones showed pro-apoptotic activity, and their apoptotic activity was not related to the number of motifs in the proteins, but was affected by the context of the motif. Based on these facts, we thought that the linkage between the motif and its phenotype would be weaker and more flexible than previously envisaged, and were interested in the possibility that the protein library constructed from a common set of peptide motifs could represent the 'promiscuous' state of the protein (22,23) (Figure 1A). In that sense, apoptotic regulatory proteins with disparate functions (a protector and a killer) may have evolved from such a promiscuous library. These considerations gave us the idea that a combinatorial library created using the BH1-4 motifs may contain both pro- and anti-apoptotic proteins that oppositely regulate the intrinsic apoptosis network (Figure 1C). We now report the functional analyses of artificial proteins in the library prepared from the BH1-4 motifs.

MATERIALS AND METHODS

Cell lines

Human cancer MCF-7 and HeLa cells were cultured at 37°C in RPMI 1640 (GIBCO) or Dulbecco's Modified Eagle's Medium (DMEM, SIGMA) respectively. The media were supplemented with 10% fetal bovine serum (FBS, JRH Biosciences) and antibiotic/antimycotic solution (A5955, Sigma). The incubator contained air enriched with 5% CO_2.

Chemicals and reagents

Staurosporine (STS) and etoposide (VP-16) were purchased from MBL and SIGMA, respectively. The mouse monoclonal c-myc antibody (Ab-1) was from Oncogene. The purified mouse anti-human PARP [poly(ADP-ribose) polymerase] (clone 7D3-6) and anti-cytochrome c (6H2.B4) monoclonal antibodies were from BD Biosciences. The rabbit polyclonal anti-Bcl-$x_{S/L}$ (S-18) and anti-Bax (N-20) antibodies were from Santa Cruz Biotechnology.

Synthesis and expressions of artificial proteins

We have recently developed a new motif programming method, which enables the combinatorial polymerization of multiple peptide motifs (12). Briefly, segments of the multiple single short DNA sequences, called microgenes$_{core}$, were first designed so that they encode the peptide motifs. These microgenes$_{core}$ were then used to create paired microgene polymerization reaction (MPR) primers. Because these primers have sequences that allow the formation of base pairs in their 3′ regions, they can stochastically recreate multiple microgenes, so that when the MPR is carried out, combinatorial polymers of multiple microgenes are generated (12). Using this method, microgenes$_{core}$, which coded BH1-4, were designed and then the MPR were carried out as previously described. The microgene polymers were cloned into one of three vectors (pcDNA 3.1/myc-His A, B or C; Invitrogen) to add a myc epitope and a poly-histidine tag at the C-terminal ends of the microgene products. Derivatives of d29 by deletion of amino acids from the N-terminus were constructed using the Kilo-sequence deletion kit (Takara). The plasmids were transfected into the MCF-7 cells or HeLa cells using lipofectamine 2000, according to the manufacturer's instructions (Invitrogen).

Screening for pro- and anti-apoptotic clones

Initially, proteins that influence the cell proliferation rate were screened using MCF-7 cells that had been plated in 96-well plates ($\sim 1 \times 10^4$ cells/well), pre-incubated for 24 h at 37°C, and then transfected with plasmids (0.16 μg) encoding the target synthetic protein. The cells' metabolic activity was assayed after 48 h by measuring the mitochondrial dehydrogenase activity using the tetrazolium salt WST-1 according to the manufacturer's (Roche) instructions. To screen for proteins that down-regulate apoptosis, the HeLa cells were plated and transfected with each plasmid (0.1 μg) as above in the presence or absence of a plasmid encoding the pro-apoptotic human Bim (50 ng). As a positive control, cells were transfected with a plasmid encoding anti-apoptotic human Bcl-xL. For all assays, a plasmid containing no synthetic component was used as the control.

Detection of apoptosis

For the TdT-mediated dUTP nick end labeling (TUNEL) assays, the MCF-7 cells were plated in 4-well permanox Lab-tek chamber slides (0.5×10^5/well; NALGE NUNC) and pre-incubated for 24 h at 37°C. After transfection with the respective plasmids (0.8 μg), the cells were incubated for 48 h and then fixed in 4% paraformaldehyde (PFA). An *in situ* Cell Death Detection Kit, Fluorescein (Roche) was then used according to the manufacturer's instructions. A plasmid encoding the pro-apoptotic human Bax served as the positive control in Figure 2. To determine the incidence of cell death shown in Figure 3, the MCF-7 cells plated in 6-well plates (1×10^6 cells/well) and pre-incubated for 24 h were transfected with the respective plasmids (4 μg) in the presence or absence of an anti-apoptotic Bcl-xL plasmid. Dead cells floating in the medium 52 h later were counted, and that number was divided by the total number of cells (1×10^6 cell/well). In Figure 4, the HeLa cells were similarly plated and transfected, after which 125 nM STS was added to the

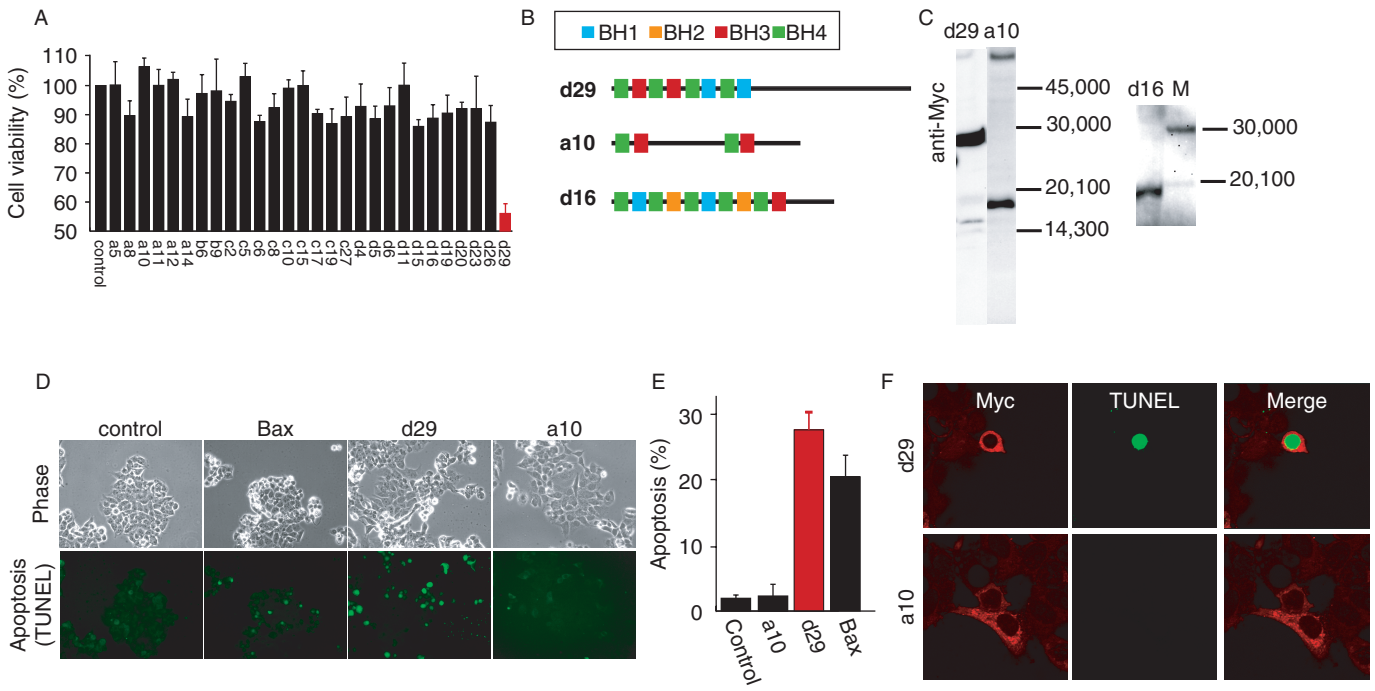

Figure 2. A pro-apoptotic clone d29 created from a mixture of BH motifs. (**A**) Screening for pro-apoptotic clones. MCF-7 cells were transfected with DNA (0.16 μg) encoding the target protein (each of 28 clones) or empty vector (control). Cell viability was then evaluated using WST-1 assays. Bars depict means ± SD from at least four independent experiments. (**B**) Schematic drawing of d29, a10 and d16 used in this study. (**C**) Expressions of d29, a10 and d16. MCF-7 cells were transfected with DNA encoding d29, a10, d16 or empty vector and analyzed by western blotting. (**D**) Pro-apoptotic function of d29. MCF-7 cells were initially transfected with DNA (0.8 μg) encoding empty vector (control), Bax, d29 or a10. After 48 h, the cells were fixed and changes in the cell morphology were correlated with TUNEL staining. (**E**) The incidence of apoptotic cells was counted using TUNEL staining. Bars depict means ± SD from three independent experiments. (**F**) Expression of synthetic proteins was visualized using a confocal microscope and anti-c-myc antibody (red). A good correlation was observed between TUNEL positivity and d29 expression.

medium and incubated for an additional 24 h. A TMR-red *in situ* Cell Death Detection Kit (Roche) was then used to detect the apoptotic cells.

Western blotting

After transfecting the resultant plasmids into MCF-7 cells plated in 6-well plates as described above, the cells were lyzed for 30 min on ice in 0.4 ml of RIPA buffer (1 × PBS, 1% NP 40, 0.5% sodium deoxycholate, 0.1% SDS, 0.1 mg/ml PMSF and 30 μl/ml aprotinin). The lyzed cells were then centrifuged at 15 000 × *g* for 20 min at 4°C, and the supernatant was used as the total cell lysate. The concentration of proteins in each sample was normalized using a DC-protein assay kit (BioRad). The membranes were incubated with the mouse monoclonal anti-c-myc antibody (1:1000, Oncogene), rabbit polyclonal anti-Bcl-xS/L antibody (1:500, Santa Cruz) or a mouse monoclonal anti-PARP antibody (1:500, BD Pharmingen).

Immunohistochemical analysis

For the immunohistochemical analysis summarized in Figure 3, cells were fixed in 4% PFA for 30 min at room temperature. The fixed cells were permeabilized in PBS containing 0.1% Triton X-100 for 3 min at 4°C, and then incubated in blocking solution (PBS with 5% goat serum and 0.3% Triton X-100) for 30 min at room temperature. The cells were then incubated first for 1 h at 37°C with the anti-cyto-c antibody (clone 6H2.B4, 1:200; Becton Dickinson), rabbit anti-c-myc antibody (1:200; SIGMA) or rabbit polyclonal anti-Bax (N-20) antibody (1:200), after which they were incubated with either the FITC-conjugated anti-mouse IgG (cytochrome-c, 1:200; ICN Pharmaceuticals) or rhodamine-conjugated anti-rabbit IgG (d29 or Bax, 1:200; Jackson Immuno Research). In Figure 4, d16 or d29 was detected by incubating the cells for 1 h at 37°C with a monoclonal mouse anti-c-myc antibody (Ab-1, 1:200; Oncogene); Bcl-xL was detected using a polyclonal rabbit anti-Bcl-xL antibody (S-18, 1:200; Santa Cruz Biotechnology). The cells were then incubated with either the FITC-conjugated anti-mouse (d16 or d29, 1:200; ICN Pharmaceuticals) or FITC-conjugated anti-rabbit (Bcl-xL, 1:100; Molecular probes) IgG. Stained samples were examined using a confocal laser scanning microscope (TCS, SP2; Leica).

RESULTS

Screening for pro-apoptotic proteins

We have recently established a new motif programming method, in which a library for artificial proteins was synthesized from the combinatorial polymerization of multiple peptide motifs (12). Using this method, we have prepared a library for artificial proteins that contained combinations of the BH1-4 motifs. In this preparation,

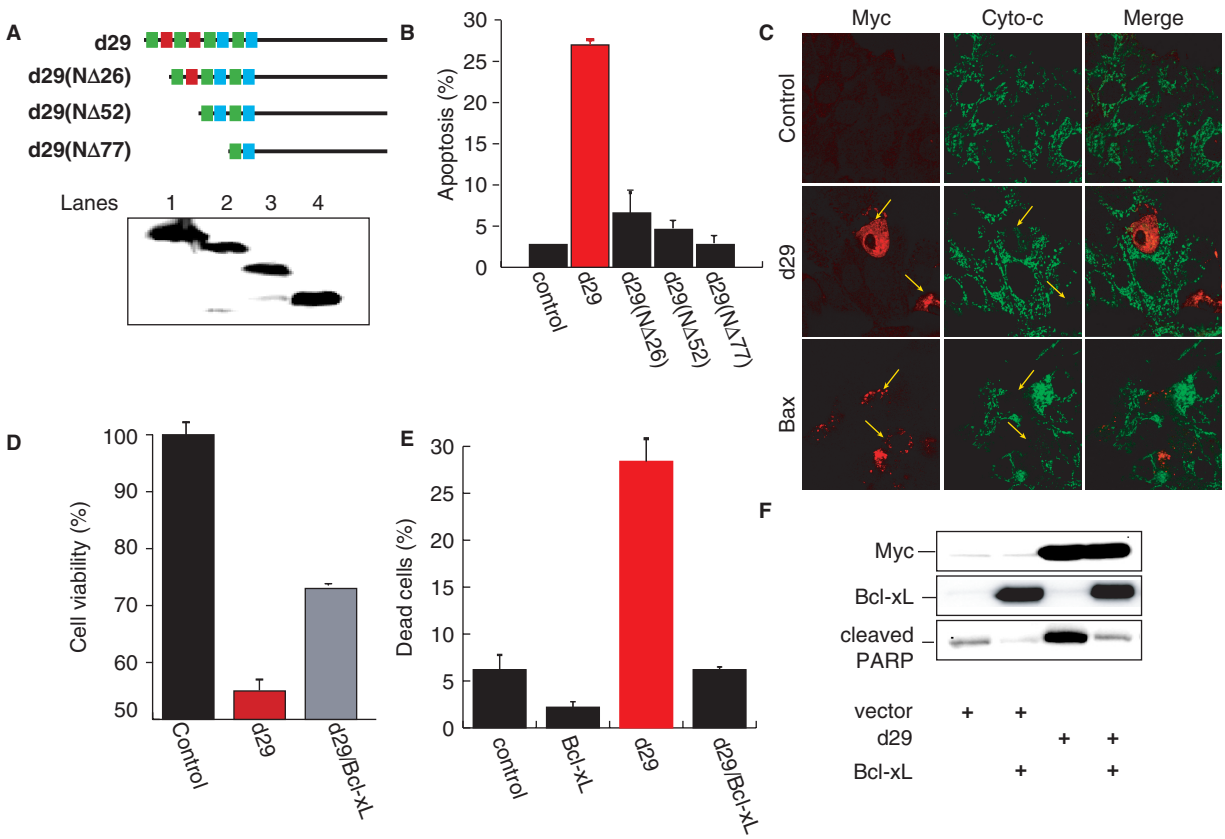

Figure 3. d29 modulates mitochondria-dependent apoptosis regulated by Bcl-xL. (**A**) Schematic drawing of mutant derivatives of d29. The lower panel shows western blots of mutants proteins expressed in MCF-7 cells detected by c-myc antibody; Lane 1; d29, Lanes 2–4; d29(NΔ26), d29(NΔ52) and d29(NΔ77). (**B**) Apoptotic inductions by d29 and its derivatives were scored by TUNEL assay. Bars depict means ± SD from three independent experiments. (**C**) Immunohistochemical analysis showing the release of cytochrome c from mitochondria in cells accumulating d29. MCF-7 cells were transfected with DNA encoding d29, Bax or empty vector (control), after which they were fixed in 4% PFA, and d29 and cytochrome c were immunostained using anti-c-myc and anti-cyto-c monoclonal antibodies, respectively. Bax was detected using anti-Bax polyclonal antibody. Cytochrome c was diffusely distributed within cells accumulating d29 or Bax, but showed a punctate distribution pattern corresponding to the mitochondria in cells not accumulating d29 or Bax. (**D**) Bcl-xL rescued cells from d29-induced growth inhibition. MCF-7 cells were transfected with DNA encoding d29, with or without a Bcl-xL expression vector. Empty vector served as a control. WST-1 assays were carried out to evaluate the cell viability. Bars depict means ± SD from three independent experiments. (**E**) MCF-7 cells were transfected as in (D). The incidence of cell death determined by counting cells floating in the medium and then dividing their number by the total number of cells (1×10^6 cell/well). Bars depict means ± SD from three independent experiments. (**F**) Bcl-xL inhibits d29-dependent PARP cleavage. Western blots of c-myc (for d29), Bcl-xL and poly (ADP-ribose) polymerase (PARP). PARP cleavage was induced by d29, and this pro-apoptotic activity was inhibited by the co-expression of Bcl-xL.

we extracted BH1, BH2 and BH4 motif (eight amino acids each) from the human Bcl-xL (anti-apoptotic) (9), and for BH3, we extracted nine amino acids from the human Noxa (pro-apoptotic) (24) ($BH1_{core}$-$BH4_{core}$, Figure 1C, middle). We used the $BH3^{Noxa}$ motif to construct a library because the simple conjugation of $BH3^{Noxa}$ and the protein transduction domain of the Tat protein (PTD^{Tat}) has been shown to penetrate into cells, but failed to induce apoptosis, whereas a combinatorial library constructed from these motifs contained bi-functional proteins (7). Among the 41 created clones, 28 (~70%) of the clones had a stable product in human cells, which was detectable by immunohistochemistry and western blot (12).

Starting from these 28 clones, we first screened for clones having pro-apoptotic activity. For this purpose, we transfected DNA for each clone to MCF-7 cells (human breast cancer cells), and scored their viability after a 48 h incubation. From this analysis, we found that the viability of the cells transfected with plasmid-d29 was reduced to 60% of that seen with the control cells transfected with the empty vector (Figure 2A). The predicted translation product, d29, was composed of 221 amino acids; it contained two $BH3_{core}$, two $BH1_{core}$ and four $BH4_{core}$ motifs, and had a myc epitope and a poly-histidine tag at its C-terminus, (Figure 2B, Supplementary Figure 1 and Table 1). We analyzed the expressions of the d29-transfected clones by western blotting and found that the predicted length of the polypeptides was detected using an anti-myc antibody (Figure 2C). An immunohistochemical analysis confirmed that the full-length of d29 was effectively expressed in human cells (Figure 2F, d29-Myc and data not shown). Thus we further characterized the function of d29. For comparison, we also examined the effects of the 139-amino acid a10 clone, which had two $BH3_{core}$ and two $BH4_{core}$ motifs, but did not appear

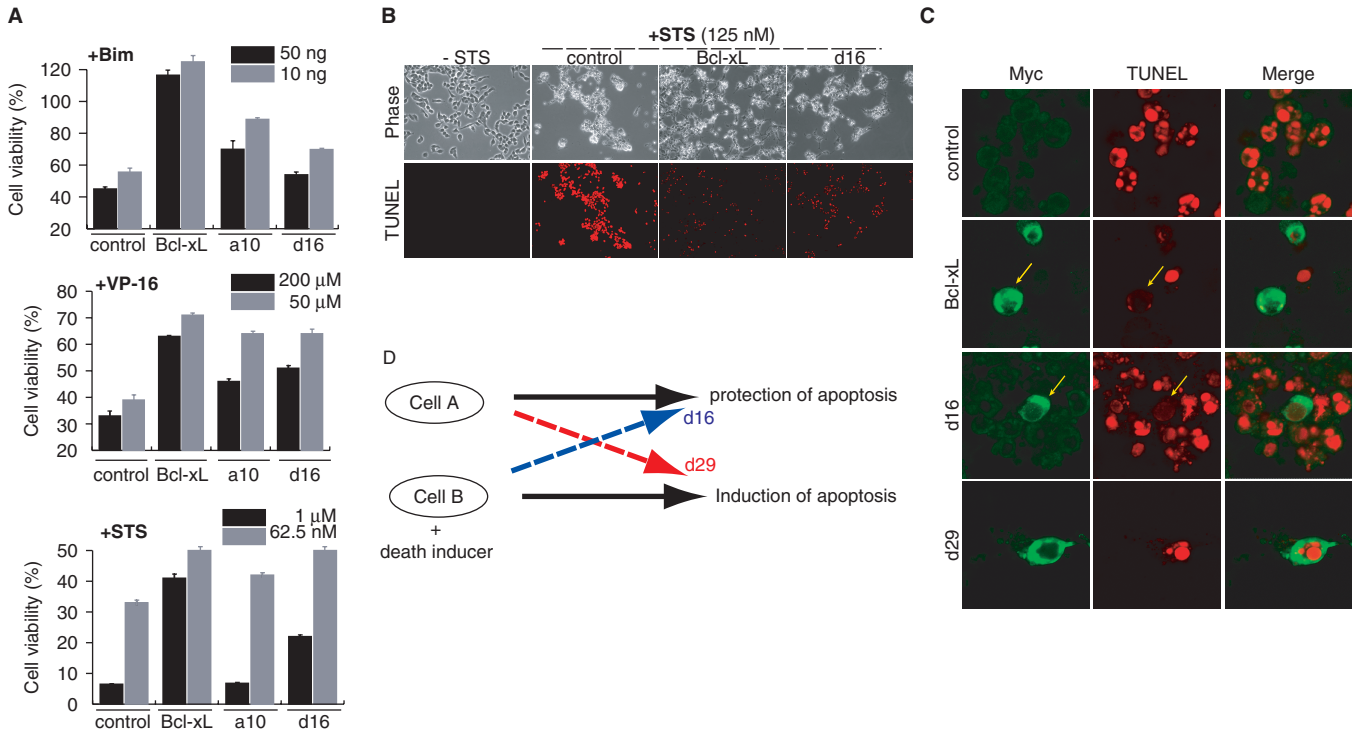

Figure 4. Anti-apoptotic d16 created from the same BH motifs-mixing library. (**A**) Transfection of clones a10 or d16 protected cells against apoptosis induced by Bim or anticancer drugs. HeLa cells transfected with DNA (0.1 μg) encoding empty vector, anti-apoptotic Bcl-xL, a10 or d16 were cotransfected with a Bim expression construct (10 or 50 ng; top) or were treated with VP-16 (50 or 200 μM; middle) or STS (62.5 or 1000 nM; bottom). Cell viability was then measured (WST-1 assays); bars depict means ± SD from three independent experiments. (**B**) Cell morphological and TUNEL analyses showing the anti-apoptotic activity of d16. (**C**) Anti-apoptotic effect of d16. Transfected HeLa cells were treated for 23 h with 125 nM STS before TUNEL analysis (red) and immunostaining of synthetic or Bcl-xL proteins (green). The same cells seen in Figure 4B were used to evaluate the correlation between the changes in the cell morphology and TUNEL staining. (**D**) Schematic diagram of two protein modulators (d29 and a10/d16) that oppositely regulate apoptotic regulatory networks.

to inhibit cell growth (Figures 2A and B, and Supplementary Figure 1), and Bax, which is known to be one of the naturally occurring pro-apoptotic Bcl-2 family proteins (Figure 1B, right).

Forty-eight hours after transfecting the respective plasmids into MCF-7 cells, ~30% of the d29-transfectants were apoptotic as indicated by their TUNEL positivity (Figure 2D). In contrast, the incidence of TUNEL positivity was less than 5% among the a10 transfectants and control vector-transfected cells. The pro-apoptotic effect of d29 was similar to that of Bax (Figure 2E, 30% versus 20%), and the morphological changes induced by the d29 transfectants were also similar to that of the Bax transfectants; cell shrinkage and condensation of the nucleus were observed (Figure 2D, phase). Immunostaining of the d29 transfectants with the anti-myc antibody revealed a good correlation between the TUNEL positivity and d29 accumulation whereas the a10 transfectants did not (Figure 2F). These results indicated that d29 induces apoptosis in a human cancer cell.

The N-terminal motifs of d29 are indispensable for the pro-apoptotic function

In order to identify the regions of d29 that are responsible for the pro-apoptotic function, we constructed three N-terminal truncated derivatives by deleting the 5′ portions of the gene (d29-NΔ26, -Δ52, -Δ77, Figure 3A). The expression levels and localizations in the MCF-7 cells were similar amongst those derivatives and d29 (Figure 3A, lanes 1–4, and data not shown). However, TUNEL staining showed that all of the d29 derivatives significantly reduced the pro-apoptotic activity that their parental d29 possesses (Figure 3B). One of the derivatives had its N-terminal 26 residues deleted, indicating that this short region containing the $BH4_{core}$ and $BH3_{core}$ motifs is indispensable for the pro-apoptotic activity of d29.

We next wondered whether d29 induced apoptosis through the mitochondria-dependent pathways. Because the release of cytochrome c from the mitochondria is an essential marker for mitochondrial-dependent apoptosis (Figure 1B), we investigated the localization pattern of cytochrome c in the d29-transfected cells. Cells transfected with the empty vector and stained with the anti-cytochrome c or Mitotracker™ exhibited overlapping punctate distributions of cytochrome c and the mitochondrial, indicating that cytochrome c remained associated with the mitochondria in the control cells (Figure 3C, top and data not shown). In contrast, the distribution of cytochrome c in cells transfected with the pro-apoptotic protein d29 or Bax (stained by anti-myc or anti-Bax antibodies) was diffuse, indicating the cytochrome c was

not tightly associated with the mitochondria in those cells (Figure 3C, middle and bottom). Thus these results suggest that the growth inhibition caused by d29 is due to the induction of the mitochondria-dependent apoptosis.

d29 modulates Bcl-xL-dependent apoptosis network

Next we investigated whether the d29-modulated apoptosis network was regulated by Bcl-2 family proteins. Although the apoptosis network in the mitochondria is not completely understood and many unknown proteins are likely to participate in this network (14), it is generally accepted that the pro-apoptotic Bcl-2 family proteins are crucially involved and that their pro-apoptotic activity is negatively modulated by the anti-apoptotic Bcl-2 family (e.g. Bcl-xL). In addition, overexpression of the anti-apoptotic Bcl-2 family proteins often inhibit apoptosis caused by the exogenous expression of the pro-apoptotic Bcl-2 family proteins, which is consistent with the idea that the relative levels of the pro- and anti-apoptotic proteins determines the cell fate in the Bcl-2 family-dependent apoptosis network (Figure 1B) (13). With that in mind, we investigated the extent to which the d29-induced apoptosis could be inhibited by the exogenous expression of Bcl-xL. We found that when MCF-7 cells were co-transfected with plasmids encoding d29 and Bcl-xL, the growth inhibitory effect of d29 was remarkably prevented (Figure 3D), and the d29-induced cell death was also attenuated; ~30% of the cells transfected with d29 alone died, as compared to <10% of the cells transfected with the d29 plus Bcl-xL (Figure 3E). We then confirmed the suppression of apoptosis in these cells by assessing the levels of the cleaved PARP, a hallmark of the activation of the executive caspases, key apoptotic mediators. As expected, the level of the cleaved PARP increased with the expression of d29 but was reduced to the control levels by co-expression of Bcl-xL (Figure 3F). To further investigate the possibility that d29 acted via Bcl-proteins pathway, we carried out co-immnoprecipitation (Co-IP) assay. From these assays, we found that Bcl-xL was co-immunoprecipitated with c-myc-tagged d29, suggesting that the interaction between d29 and Bcl-xL was involved in the d29-induced apoptosis (Supplementary Figure 2A). The d29 also induced reduction of mitochondrial transmembrane potential ($\Delta\psi_m$) in a similar manner to the pro-apoptotic Bax, and loss of $\Delta\psi_m$ induced by d29 was partially reversed by Bcl-xL overexpression. These results confirmed that d29 modulated Bcl-xL function and then activated Bcl-2 family-dependent apoptosis pathways (Supplementary Figure 2B). Therefore, it appears that d29 crosstalks with the intrinsic apoptosis circuits regulated by Bcl-xL and thus the pro-apoptotic function of d29 reflects its ability to modulate the apoptosis signaling networks composed of the Bcl-2 family proteins.

Anti-apoptotic proteins generated from the same library

To determine whether the above protein library generated by motif programming also contained anti-apoptotic proteins, we scored the capacity of the 28 clones to relieve the growth inhibition caused by the naturally occurring pro-apoptotic protein, Bim (25) (Figure 1B). In this experiment, we used HeLa cells instead of MCF-7 cells because Bcl-xL did not efficiently suppress the pro-apoptotic activity of Bim in the MCF-7 cells, but did so in HeLa cells (data not shown). The pro-apoptotic effect of the d29 transfectant was also confirmed in the HeLa cells (Figure 4C, d29, and data not shown). When we transfected the HeLa cells with Bim alone, the cell viability was only ~40–60% of that seen with the control cells (Figure 4A, + Bim). Interestingly, two clones (a10 and d16, Figure 2B and Supplementary Figure 1) have been screened for a potent anti-apoptotic modulator, because the a10 or d16 plus Bim transfectants increased the viability to 60–80% of the control cells under various conditions, but the 26 other clones did not. (Figure 4A, + Bim and data not shown). Because it has been reported that the exogenous expression of Bcl-xL effectively suppresses the apoptosis caused by anti-cancer drugs and pro-apoptotic proteins, we also compared the effects of Bcl-xL to those of a10/d16 on the viability among the cells treated with VP-16 or STS, which are known to induce mitochondria-dependent apoptosis. Treating HeLa cells transfected with an empty vector with either of the drugs markedly reduced the viability, but the cell viability was partially restored by transfection of a10 or d16 (Figure 4A, + VP-16 and + STS), although the anti-apoptotic activities of a10/d16 were moderate compared to that of Bcl-xL. We further analyzed the apoptosis-inhibitory effect of d16. The d16 protein was composed of 164 amino acids and contained all of the BH1-4 motifs (two $BH1_{core}$, two $BH2_{core}$, one $BH3_{core}$, and five $BH4_{core}$) (Figure 2B). We analyzed the expressions of the d16-transfected clones and confirmed that the predicted lengths of the polypeptides were detected (Figure 2C).

The anti-apoptotic effect of the d16 transfectant was confirmed by TUNEL assays of the STS-treated cells. A strong TUNEL signal (rhodamine fluorescence; red) was observed when the cells were transfected with the empty vector and then incubated for 23 h with 125 nM STS, but that the signal was significantly diminished by transfection of Bcl-xL or d16 (Figure 4B). In addition, immunostaining with the anti-myc (for d16) or anti-Bcl-xL antibody together with TUNEL showed that cells expressing Bcl-xL or d16 were protected from the STS-induced apoptosis (Figure 4C, Bcl-xL/d16, shown by yellow arrows), which is consistent with the anti-apoptotic activities of these proteins. We also investigated the involvement of Bcl pathway in the anti-apoptotic activities of a10 and d16. It is known that Bax activation (the oligomerization of Bax) is essential for Bcl-2 family-dependent pathway. The oligomerization state of Bax was determined by cross-linking and subsequent immunoblot analysis. We confirmed that a10/d16 modulated Bax-dependent apoptosis pathways; Bax-transfected cells induced Bax oligomerization, but the levels of Bax oligomerization were reduced in Bax and a10 (d16)-co-transfected cells (Supplementary Figure 2C). These confirmed that a10/d16 also act via Bcl-2 family-dependent apoptosis pathways. Taken together, our findings indicate that both the pro-apoptotic (d29) and anti-apoptotic (a10/d16) proteins can be generated

from a single library composed of a combinatorial assemblage of four BH1-4$_{core}$ motifs (Figure 4D).

Diverse subcellular localizations generated by motif programming

It has been reported that the Bcl-2 family proteins are localized in a variety of cellular organelles even though they share the same BH motifs (21). For instance, the anti-apoptotic Bfl-1S and Bcl-xL, both of which contained the BH1-4 motifs, mainly localize in the nucleus and mitochondria, respectively (26). To investigate whether different arrangements of the BH$_{core}$ motifs affect the subcellular localizations of artificial proteins, we monitored the localizations of all of the 28 clones and interestingly found that these proteins are localized in a variety of organelles, including the nucleus, cytoplasm or mitochondria (Figure 5 and summarized in Table 1). This suggests that the artificial proteins were effectively expressed and formed stable products in cells, and then translocated to the various intracellular compartments. We have previously reported that the a8 protein exhibits overlapping distributions with mitochondria (12). Three other clones (a10, a12 and a14) also appeared to be localized in the mitochondria, because Mitotracker™ merged with the localization patterns of these proteins (Figure 5, top, and data not shown). However, these proteins did not include naturally occurring mitochondria targeting motifs (Supplementary Figure 1). The b6, b9, c2, c8 and d5 proteins are localized in the nucleus whereas the other proteins seemed to be localized in the cytoplasm (Figure 5, middle and bottom). Thus the localizations of proteins were dependent on how the microgenes were joined together and how the reading frames appeared on the microgene polymers (Supplementary Figure 1 and Table 1). Although further structural and mutational analyses will be necessary to fully elucidate the roles of BH1-4$_{core}$ in the functions as well as localizations of these proteins, it would be noteworthy that synthetic proteins with different function/localization patterns can emerge from a single pool prepared from common peptide motifs.

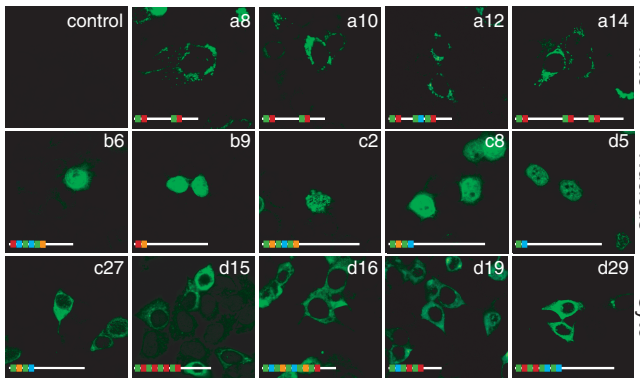

Figure 5. Investigating the relationship between protein sequences and cellular localizations. For analysis of the protein localizations, the MCF-7 cells were plated and pre-incubated for 24 h at 37°C. After transfection with the respective plasmids (0.8 μg) using lipofectamine (2 μl), the cells were incubated for 24 h and then fixed in 4% PFA. The localizations of the synthetic proteins were analyzed using the anti-myc antibody (see also Materials and Methods section for Immunohistochemical Analysis). Schematic drawing of artificial proteins is also shown.

DISCUSSION

Motifs are generally identified as evolutionally conserved sequences in the primary structures of proteins (27). As their identities have remained during the course of evolution, motifs must have certain biological functions. In proteins involved with signal transductions, motifs

Table 1. Properties of artificial proteins used in this study

Name	Total residues	Mw	pI	Amino acid composition		Localization
				Positive[a]	Negative[b]	
d29	221	24 655	9.43	0.14	0.12	Cytoplasm
d29NΔ26	195	21 585	8.39	0.13	0.12	Cytoplasm
d29NΔ52	169	18 516	6.49	0.11	0.12	Cytoplasm
d29NΔ77	144	15 580	6.74	0.10	0.10	Cytoplasm
a10	139	15 642	11.17	0.19	0.10	Mitochondria/cytoplasm
d16	164	19 183	9.48	0.16	0.15	Cytoplasm
a8	142	16 062	10.79	0.18	0.10	Mitochondria
a12	140	15 642	10.7	0.19	0.14	Mitochondria
a14	242	26 356	10.87	0.15	0.09	Mitochondria
b6	142	16 836	6.8	0.15	0.16	Nucleus/ cytoplasm
b9	164	19 058	11.82	0.21	0.08	Nucleus/ cytoplasm
c2	217	23 070	5.61	0.08	0.11	Nucleus /cytoplasm
c8	216	23 935	11.28	0.16	0.10	Nucleus/ cytoplasm
d5	193	22 098	11.86	0.21	0.08	Nucleus
c27	168	18 159	6.75	0.12	0.13	Cytoplasm
d15	171	19 716	10.8	0.19	0.11	Cytoplasm
d19	117	13 675	10.76	0.19	0.13	Cytoplasm

Molecular weights (Mw) were calculated from nucleotide sequences. Isoelectric points (pI) were calculated by ProtParam tool (http://au.expasy.org/tools/protparam.html).
[a]Lys and Arg.
[b]Asp and Glu.

are often related to the sites for protein–protein interaction (9,10), which underlie the complex, dynamic and robust protein network (28).

Our motif programming is a method for creating multifunctional proteins by virtue of the linkage between motifs and their functions, i.e. realizing new combinations of functions by combining motifs whose functions have been already annotated (7,12,29,30). What we learned from our past motif programming studies can be summarized as follows: (i) tight protein folding is not necessary for the expression of functions and (ii) expression of the motif function is influenced by the context of the motif. We used our MolCraft (31) and its modified method in the motif programming experiments (7,32,33). In this methodology, motifs are embedded in different reading frames of a microgene or different microgenes, and the motifs are combinatorially assembled to make the protein library. Proteins created from these methods are usually disordered and not tightly folded, although they often exhibit secondary structures (30). Nevertheless, we observed that some of these artificial proteins exerted biological functions such as cell penetration, apoptosis and biomineralization (7,34). Thus, tight folding is not necessary for a protein to express (at least some of) biological functions.

Motif programming is the rational design of artificial proteins. However, proteins containing embedded motifs do not always possess the designed functions. For instance, when the cell-penetrating motif PTD and apoptosis-inducing motif BH3 were programmed to make bifunctional proteins, a fraction of the clones in the library showed distinct functions of cell penetrating and apoptosis inducing (7). Most of them have moderate function(s) irrespective of the contained motifs. The strong expression of functions was not result from multiplicities of the motif. Apparently, their functional expression was influenced by where the motifs were located in the proteins, i.e. influenced by the context of the motif. Similar capriciousness has been observed in our or others' motif-based experiments (8). Thus, the function annotated to the motifs seems to be no longer a mere absolute when they are detached from their parental bodies. Motifs must be in a promiscuous state in terms of function.

These observations prompted us to investigate the properties of the artificial library that we have prepared from the BH1-4 motifs. The protein networks that regulate the mitochondrial apoptosis contain combinations of the BH1-4 motifs, and form a complex network from various components. Although bewildering factors are involved, the general principle is rather simple, that is, the balance between the pro-apoptotic and anti-apoptotic proteins determine the cell fate, i.e. either cell survival or death. For instance, the function of the pro-apoptotic Bim was attenuated by the ectopic expression of the anti-apoptotic Bcl-xL (25). With these situations in mind, we investigated how our 28 artificial clones, which have been created by assembling the BH1-4 motifs, would influence the intrinsic apoptosis signaling network. We observed that the d29 clone showed a strong pro-apoptotic activities and a10 and d16 showed a moderated, but unambiguous anti-apoptotic activity. We clearly found that the pro-apoptotic activity of d29 was significantly attenuated by the overexpression of Bcl-xL. Conversely, the anti-apoptotic effect of a10/d16 partially blocked the effect of the pro-apoptotic Bim and anti-cancer drugs (STS or VP-16) in a manner similar to Bcl-xL. Thus, disparate functions (a cell killer and a cell protector) have emerged from a single pot of a protein library. Because the existence of motifs in these clones was not linked to their phenotypes, we believed that the promiscuous state of a protein was realized in a motif-shuffling library. Our finding suggests that peptide motifs contributed to the accomplishment of the plastic evolvability of the protein network.

SUPPLEMENTARY DATA

Supplementary Data are available at NAR Online.

ACKNOWLEDGEMENTS

We thank T. Mashima for helpful discussions. T. Minamisawa, K. Hayashi and R. Furushima for DNA cloning, flow cytometry and immunoblot analyses, S. Shimizu and Y. Shirakata for providing the Bax and Bcl-xL expression plasmids, and T. Nakamura and D. Huang for providing the Bim expression plasmid. This study was supported in part by a Grant-in-Aid for Scientific Research from Ministry of Education, Science, Sports and Culture, Japan. H.S. acknowledges Grant-in-Aid for Young Scientists (A). Funding to pay the Open Access publication charges for this article was provided by Japan Science and Technology Agency.

Conflict of interest statement. None declared.

REFERENCES

1. Kitano,H. (2004) Biological robustness. *Nat. Rev. Genet*., **5**, 826–837.
2. Stelling,J., Sauer,U., Szallasi,Z., Doyle,F.J.III and Doyle,J. (2004) Robustness of cellular functions. *Cell*, **118**, 675–685.
3. Patthy,L. (1985) Evolution of the proteases of blood coagulation and fibrinolysis by assembly from modules. *Cell*, **41**, 657–663.
4. King,N., Hittinger,C.T. and Carroll,S.B. (2003) Evolution of key cell signaling and adhesion protein families predates animal origins. *Science*, **301**, 361–363.
5. Neduva,V., Linding,R., Su-Angrand,I., Stark,A., de Masi,F., Gibson,T.J., Lewis,J., Serrano,L. and Russell,R.B. (2005) Systematic discovery of new recognition peptides mediating protein interaction networks. *PLoS Biol*., **3**, e405.
6. Edwards,R.J., Moran,N., Devocelle,M., Kiernan,A., Meade,G., Signac,W., Foy,M., Park,S.D., Dunne,E. *et al.* (2007) Bioinformatic discovery of novel bioactive peptides. *Nat. Chem. Biol*., **3**, 108–112.
7. Saito,H., Honma,T., Minamisawa,T., Yamazaki,K., Noda,T., Yamori,T. and Shiba,K. (2004) Synthesis of functional proteins by mixing peptide motifs. *Chem. Biol*., **11**, 765–773.
8. Frugier,M., Giege,R. and Schimmel,P. (2003) RNA recognition by designed peptide fusion creates "artificial" tRNA synthetase. *Proc. Natl Acad. Sci. USA*, **100**, 7471–7475.
9. Sattler,M., Liang,H., Nettesheim,D., Meadows,R.P., Harlan,J.E., Eberstadt,M., Yoon,H.S., Shuker,S.B., Chang,B.S. *et al.* (1997) Structure of Bcl-xL-Bak peptide complex: recognition between regulators of apoptosis. *Science*, **275**, 983–986.
10. Pawson,T. and Nash,P. (2003) Assembly of cell regulatory systems through protein interaction domains. *Science*, **300**, 445–452.

11. Dueber,J.E., Yeh,B.J., Bhattacharyya,R.P. and Lim,W.A. (2004) Rewiring cell signaling: the logic and plasticity of eukaryotic protein circuitry. *Curr. Opin. Struct. Biol.*, **14**, 690–699.
12. Saito,H., Minamisawa,T. and Shiba,K. (2007) Motif programming: a microgene-based method for creating synthetic proteins containing multiple functional motifs. *Nucleic Acids Res.*, **35**, e38.
13. Opferman,J.T. and Korsmeyer,S.J. (2003) Apoptosis in the development and maintenance of the immune system. *Nat. Immunol.*, **4**, 410–415.
14. Green,D.R. (2005) Apoptotic pathways: ten minutes to dead. *Cell*, **121**, 671–674.
15. Strasser,A. (2005) The role of BH3-only proteins in the immune system. *Nat. Rev. Immunol.*, **5**, 189–200.
16. Shimizu,S., Konishi,A., Kodama,T. and Tsujimoto,Y. (2000) BH4 domain of antiapoptotic Bcl-2 family members closes voltage-dependent anion channel and inhibits apoptotic mitochondrial changes and cell death. *Proc. Natl Acad. Sci. USA*, **97**, 3100–3105.
17. Letai,A., Bassik,M.C., Walensky,L.D., Sorcinelli,M.D., Weiler,S. and Korsmeyer,S.J. (2002) Distinct BH3 domains either sensitize or activate mitochondrial apoptosis, serving as prototype cancer therapeutics. *Cancer Cell*, **2**, 183–192.
18. Moreau,C., Cartron,P.F., Hunt,A., Meflah,K., Green,D.R., Evan,G., Vallette,F.M. and Juin,P. (2003) Minimal BH3 peptides promote cell death by antagonizing anti-apoptotic proteins. *J. Biol. Chem.*, **278**, 19426–19435.
19. Walensky,L.D., Kung,A.L., Escher,I., Malia,T.J., Barbuto,S., Wright,R.D., Wagner,G., Verdine,G.L. and Korsmeyer,S.J. (2004) Activation of apoptosis in vivo by a hydrocarbon-stapled BH3 helix. *Science*, **305**, 1466–1470.
20. Lin,B., Kolluri,S.K., Lin,F., Liu,W., Han,Y.H., Cao,X., Dawson,M.I., Reed,J.C. and Zhang,X.K. (2004) Conversion of Bcl-2 from protector to killer by interaction with nuclear orphan receptor Nur77/TR3. *Cell*, **116**, 527–540.
21. Portier,B.P. and Taglialatela,G. (2006) Bcl-2 localized at the nuclear compartment induces apoptosis after transient overexpression. *J. Biol. Chem.*, **281**, 40493–40502.
22. James,L.C. and Tawfik,D.S. (2001) Catalytic and binding poly-reactivities shared by two unrelated proteins: the potential role of promiscuity in enzyme evolution. *Protein Sci.*, **10**, 2600–2607.
23. Aharoni,A., Gaidukov,L., Khersonsky,O., Mc,Q.G.S., Roodveldt,C. and Tawfik,D.S. (2005) The 'evolvability' of promiscuous protein functions. *Nat. Genet.*, **37**, 73–76.
24. Oda,E., Ohki,R., Murasawa,H., Nemoto,J., Shibue,T., Yamashita,T., Tokino,T., Taniguchi,T. and Tanaka,N. (2000) Noxa, a BH3-only member of the Bcl-2 family and candidate mediator of p53-induced apoptosis. *Science*, **288**, 1053–1058.
25. O'Connor,L., Strasser,A., O'Reilly,L.A., Hausmann,G., Adams,J.M., Cory,S. and Huang,D.C. (1998) Bim: a novel member of the Bcl-2 family that promotes apoptosis. *EMBO J.*, **17**, 384–395.
26. Ko,J.K., Lee,M.J., Cho,S.H., Cho,J.A., Lee,B.Y., Koh,J.S., Lee,S.S., Shim,Y.H. and Kim,C.W. (2003) Bfl-1S, a novel alternative splice variant of Bfl-1, localizes in the nucleus via its C-terminus and prevents cell death. *Oncogene*, **22**, 2457–2465.
27. Neduva,V. and Russell,R.B. (2005) Linear motifs: evolutionary interaction switches. *FEBS Lett.*, **579**, 3342–3345.
28. Lanave,C., Santamaria,M. and Saccone,C. (2004) Comparative genomics: the evolutionary history of the Bcl-2 family. *Gene*, **333**, 71–79.
29. Shiba,K., Takahashi,Y. and Noda,T. (1997) Creation of libraries with long ORFs by polymerization of a microgene. *Proc. Natl Acad. Sci. USA*, **94**, 3805–3810.
30. Shiba,K., Takahashi,Y. and Noda,T. (2002) On the role of periodism in the origin of proteins. *J. Mol. Biol.*, **320**, 833–840.
31. Shiba,K. (2004) Molcraft: a hierarchical approach to the synthesis of artificial proteins. *J. Mol. Catal. B.*, **28**, 145–153.
32. Kashiwagi,K. and Shiba,K. (2004) Combinatorics of peptide sextets encoded by a single microgene. *J. Mol. Catl. B.*, **28**, 215–221.
33. Kashiwagi,K., Isogai,Y., Nishiguchi,K. and Shiba,K. (2006) Frame shuffling: a novel method for *in vitro* protein evolution. *Protein Eng. Des. Sel.*, **19**, 135–140.
34. Shiba,K., Honma,T., Minamisawa,T., Nishiguchi,K. and Noda,T. (2003) Distinct macroscopic structures developed from solutions of chemical compounds and periodic proteins. *EMBO Rep.*, **4**, 148–153.